Title

Destabilizing the autoinhibitory conformation of Zap70 induces up-regulation of inhibitory receptors and T cell unresponsiveness.

Journal

The Journal of experimental medicine, 214(3)

ISSN

0022-1007

Authors

Hsu, Lih-Yun
Cheng, Debra A
Chen, Yiling
et al.

Publication Date

2017-03-01

DOI

10.1084/jem.20161575

Peer reviewed

Destabilizing the autoinhibitory conformation of Zap70 induces up-regulation of inhibitory receptors and T cell unresponsiveness

Lih-Yun Hsu,[1,2] Debra A. Cheng,[1,2] Yiling Chen,[1,2] Hong-Erh Liang,[2] and Arthur Weiss[1,2]

[1]Department of Medicine, Rosalind Russell and Ephraim Engleman Rheumatology Research Center and [2]Howard Hughes Medical Institute, University of California, San Francisco, CA 94143

Zap70 plays a critical role in normal T cell development and T cell function. However, little is known about how perturbation of allosteric autoinhibitory mechanisms in Zap70 impacts T cell biology. Here, we analyze mice with a hypermorphic Zap70 mutation, W131A, which destabilizes the autoinhibitory conformation of Zap70, rendering the kinase in a semiactive state. W131A mutant mice with wild-type T cell receptor (TCR) repertoires exhibited relatively normal T cell development. However, crossing the W131A mutant mice to OTII TCR transgenic mice resulted in increased negative selection of OTII$^+$ thymocytes and in increased thymic and peripheral T regulatory cells. Strikingly, increased basal TCR signaling was associated with a marked increase in inhibitory receptor expression and with T cells that were relatively refractory to TCR stimulation. PD-1 inhibitory receptor blockade partially reversed T cell unresponsiveness. Collectively, disruption of normal Zap70 autoinhibition engaged negative feedback mechanisms by which negative selection and inhibitory receptors restrain TCR signaling to enforce both central and peripheral tolerance.

The Journal of Experimental Medicine

INTRODUCTION

TCR signaling during thymic development directs critical cell fate decisions that select a functional, self-tolerant, and diverse T cell repertoire. The mature T cell repertoire is largely determined at the CD4CD8 double-positive (DP) thymocyte stage, dictated by the affinity of the interaction between the TCR and self-peptides bound to MHC (pMHC) molecules. Low affinity interactions generate signals that promote survival and maturation to the CD4 or CD8 single-positive (SP) stages of thymocyte development, whereas high affinity interactions of the TCR with pMHC generate signals leading to cell death by negative selection. Additionally, several CD4SP thymocytes receiving relatively strong signals through their TCRs escape deletion and differentiate into regulatory T (T reg) cells (Starr et al., 2003; Hogquist and Jameson, 2014). Thus, the signaling intensity of the TCR signal must be properly regulated to be reflective of its recognition of pMHC.

The signal transduction machinery downstream of TCR and its regulation play important roles in the various thymocyte developmental outcomes and in peripheral T cell responses. One of the key proteins of the TCR signaling machinery is Zap70, a cytoplasmic tyrosine kinase. The importance of Zap70 is highlighted by loss-of-function mutations, which lead to impaired T cell development and immune deficiency states in mice and in humans (Wang et al., 2010). Hypomorphic alleles can lead to systemic autoimmune disease phenotypes (Sakaguchi et al., 2003; Siggs et al., 2007). In addition to Zap70, the Src family kinase Lck is critical to TCR signaling. Lck initiates TCR downstream signaling events by phosphorylating paired tyrosines in the immunoreceptor tyrosine-based activation motifs (ITAMs) of the CD3 and ζ chains, as well as by phosphorylating and activating Zap70. The full activation of Zap70 initiates TCR downstream signals that depend on its phosphorylation of two adaptor proteins, linker of activated T cells (LAT) and SLP-76, which are required for increases in intracellular calcium and activation of the Ras–MAP kinase pathway (Smith-Garvin et al., 2009).

The proper regulation of Zap70 activity is critically important. In the ITAM-unbound state, Zap70 is presumed to be in an autoinhibited conformation in the cytoplasm. The crystal structure of nonphosphorylated Zap70 has revealed the basis of this autoinhibited conformation (Deindl et al., 2007, 2009; Yan et al., 2013). Its N-terminal tandem SH2 domains are misaligned for ITAM binding and are separated by interdomain A, which forms three helices behind the SH2 domains that interact with the back of the inactive conformation of the kinase domain and with sequences in interdomain B that links the C-terminal SH2 domain to the N-lobe of the kinase domain. Interdomain B contains two tyrosines, Y315 and Y319, which participate in Zap70 autoinhibition. In their unphosphorylated states, Y315 participates in hydrophobic interactions with W131 in interdomain A, whereas Y319 interacts with the N-lobe of the catalytic domain (Yan

Correspondence to Arthur Weiss: aweiss@medicine.ucsf.edu

Abbreviations used: DP, double-positive; ITAM, immmunoreceptor tyrosine-based activation motif; LAT, linker of activated T cells; SP, single-positive; tg, transgenic.

The Rockefeller University Press $30.00
J. Exp. Med. 2017 Vol. 214 No. 3 833–849
https://doi.org/10.1084/jem.20161575

et al., 2013). These hydrophobic interactions involving these two tyrosines are essential for full autoinhibition. Phosphorylation of these tyrosines by Lck is important for stabilizing the active conformation of the kinase and for the recruitment of important effector molecules.

For normal function of Zap70, the autoinhibited conformation is believed to be relieved in two steps based on mutagenesis studies and by recent hydrogen-deuterium exchange studies (Brdicka et al., 2005; Deindl et al., 2009; Yan et al., 2013; Klammt et al., 2015). The first step occurs when Zap70 is recruited to the TCR complex via high affinity interaction of its tandem N-terminal SH2 domains with doubly phosphorylated ITAMs. The alignment of the tandem SH2 domains upon phospho-ITAM binding is associated with a rotation and straightening of two of the helices in interdomain A, which is predicted to destabilize interactions between W131 and Y315 and other hydrophobic interactions, leading to increased accessibility of Y315 and Y319 to Lck. These latter events enable the second step of activation, in which Lck phosphorylates Y315 and Y319 in interdomain B, as well as Y493 in the activation loop of catalytic domain. The second step results in the adoption of the catalytically active conformation and full activation of the Zap70 kinase. This discrete two-step process of activation likely explains the finding of unphosphorylated Zap70 being bound to phosphorylated TCR ζ chain ITAMs in ex vivo thymocytes and T cells, a consequence of TCR interactions with endogenous self-pMHC molecules (van Oers et al., 1994; Witherden et al., 2000; Mandl et al., 2013; Persaud et al., 2014). Thus, recruitment of Zap70 to the TCR can precede its full activation.

The importance of the autoinhibited conformation is highlighted by the Lck-independent activation of Zap70 in heterologous 293T cells or with recombinant proteins when either Y315 and Y319 or W131 are mutated to alanine (Deindl et al., 2007, 2009). Expression of the W131A mutant in Zap70-deficient Jurkat cells results in hyperresponsiveness to TCR stimulation. Therefore, the autoinhibited conformation could safeguard the T cell from inappropriate activation that could lead to autoimmunity. Indeed, a recent report of a family with two affected children with profound multisystem, tissue-specific autoimmune disease showed disease resulted from inheritance of a hypomorphic mutation and a weak hypermorphic mutation in Zap70 that destabilized the autoinhibited conformation by disrupting the interaction of Y319 with the N-lobe of the kinase (Chan et al., 2016). However, mechanistic insights into how the combination of the hypomorphic and the activating mutants of Zap70 lead to autoimmune disease is unclear. Further, no in vivo investigations of how a Zap70-activating allele influences thymic selection and immune tolerance mechanisms have been performed.

In this study, we examined the importance of Zap70 autoinhibition in T cell development and in T cell function by destabilizing the autoinhibitory conformation of Zap70. We generated Zap70 W131A mutant mice carrying this semi-active Zap70 kinase. When introduced into the OTII TCR transgenic (tg) background, the W131A mutation led to thymocyte negative selection and resulted in impaired peripheral T cell signaling and responses. The hyporesponsiveness of peripheral T cells in W131AOTII mice shared features with T cell anergy, as indicated by increased expression of several anergy-related genes. Striking induction of inhibitory receptors in W131AOTII T cells at least partially accounted for the peripheral T cell hyporesponsiveness. Together, these findings highlight the importance of autoinhibition of Zap70 and provide insights into how negative regulatory mechanisms induced to compensate for increased TCR signaling can also lead to T cell hyporesponsiveness.

RESULTS

Relatively normal T cell development in the Zap70 W131A mice

To examine the importance of Zap70 autoinhibition in TCR signaling, we generated a knock-in mouse with the *W131A* mutation in interdomain A of the *zap70* gene (Fig. 1 A). By intracellular staining, we found that the W131A substitution caused an ∼50% reduction of Zap70 protein in the thymocytes and peripheral T cells of homozygous W131A mice (unpublished data). Despite lower Zap70 expression in W131A mice, T cell numbers and development were comparable in young WT and W131A mice (Fig. 1, B and C). There were no substantial differences in overall cellularity in the thymi, spleens, and LNs in W131A mice relative to WT littermates (Fig. 1 C and not depicted). However, we consistently noted an increase in the CD4 T effector/memory ($CD62L^{low}CD44^{high}$) cell population in young W131A mice that increased in older mice (Fig. 1 D). In addition, W131A mice had more peripheral $Foxp3^+$ T reg cells than did their age-matched wild-type littermates (Fig. 1 E). This moderate increase in T reg cells occurred irrespective of age (range from 6 wk to 8 mo; Fig. 1 E). However, no increase in thymic T reg cells was noted (unpublished data).

We next assessed whether TCR-induced downstream signaling events and activation responses were altered in W131A T cells. Direct characterization of Zap70 and LAT phosphorylation did not reveal substantial differences in anti-CD3-induced phosphorylation of either protein (unpublished data). In addition, both W131A and WT T cells had similar kinetics and amplitudes of calcium increases and ERK phosphorylation in response to varying doses of anti-CD3 stimulation (Fig. 1, F and G). Moreover, downstream activation responses of W131A primary T cells to TCR stimulation, such as CD69 up-regulation, appeared unaffected in comparison with WT T cells (unpublished data). Collectively, our findings suggest that in mice with a polyclonal TCR repertoire, the W131A mutation was associated with no detectable changes in T cell development and no obvious impairment in TCR-induced activation, although there were increases in peripheral T reg cells and memory/effector cells over time.

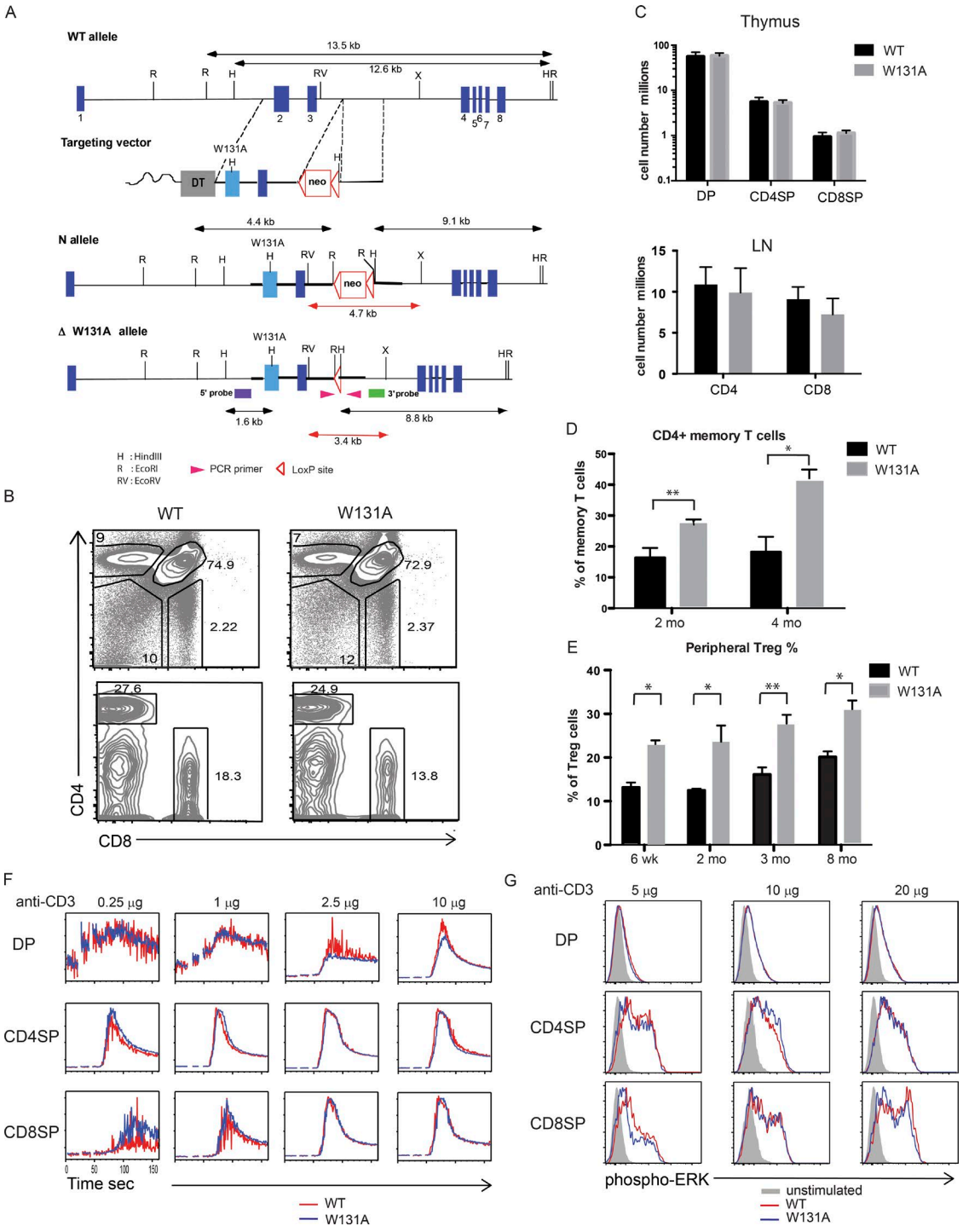

Figure 1. **W131A mice with a polyclonal TCR repertoire have grossly normal T cell development and TCR signaling.** (A) Targeting strategy used to produce W131A knock-in mice. Residue W131A present in exon 2 was mutated to alanine. (B) CD4 versus CD8 profiles of thymocytes (top) and LN cells (bottom) from WT and W131A mice. Numbers in quadrants are the percentages of each T cell subset. Results are representative of seven experiments. (C) Total cell numbers in thymi (top) and LN (bottom) in age-matched 2-mo-old WT and W131A mice. (D) Increased percentages of memory ($CD62L^{lo}CD44^{hi}$) $CD4^+$ T cells in W131A mice ($n = 5$ per group). All error bars represent SEM. *, $P < 0.05$; **, $P < 0.01$. (E) Comparison of $CD4^+Foxp3^+$ T cells from LNs of WT and W131A mice of the indicated ages ($n = 4$ per group). (F) Anti-CD3-induced calcium changes in DP thymocytes (top), CD4SP (middle), and CD8SP thymocytes (bottom) from WT and W131A mice. (G) DP, CD4SP, and CD8SP thymocytes from WT or W131A mice were analyzed for levels of phospho-ERK by flow cytometry. Unstimulated T cells (filled gray) and anti-CD3–stimulated T cells (2.5 min) from WT mice (red line), and W131A (blue line) are shown. Data are representative of three experiments.

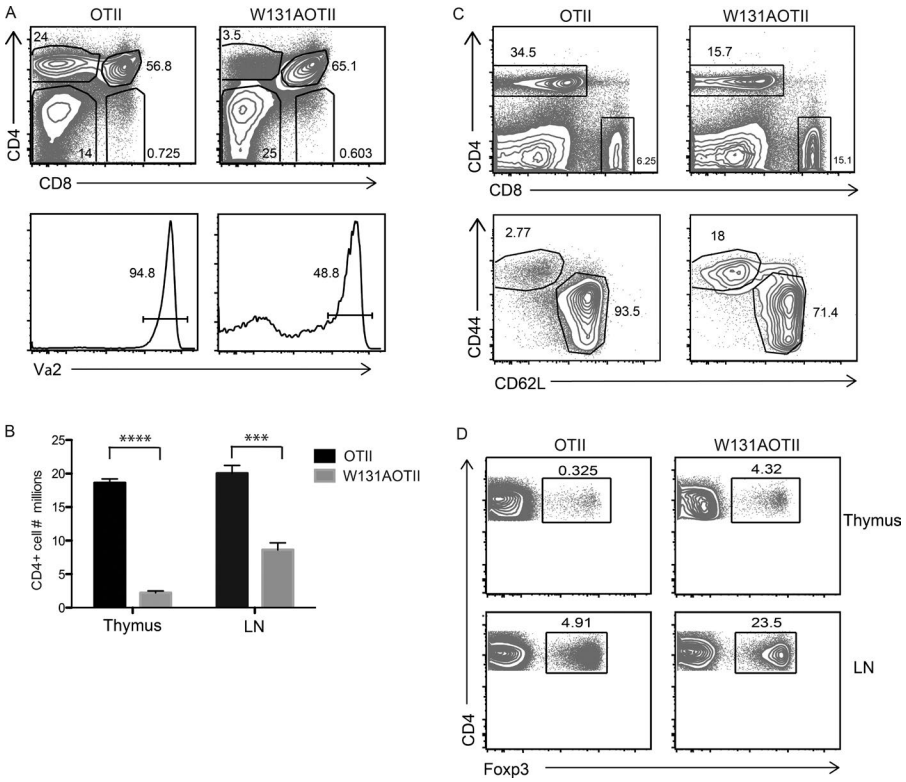

Figure 2. **Restricting the TCR repertoire in W131A mice leads to a profound impairment in T cell development.** (A) Representative plots showing expression of CD4/CD8 (top) and OTII TCR tg (bottom) in total thymocytes from OTII and W131AOTII mice. Numbers in each histogram of the bottom panels indicate the frequency of OTII (Vα2$^+$) tg-positive cells in CD4SP thymocytes. (B) Absolute numbers of CD4$^+$ T cells from thymi and LNs of either OTII or W131AOTII are shown (n = 10 per genotype). All error bars represent SEM. ***, P < 0.001; ****, P < 0.0001. (C) Representative plots showing expression of CD4/CD8 (top) and CD62L/CD44 (bottom) in LN cells from OTII and W131AOTII mice. (D) Representative flow cytometric profiles of CD4 and Foxp3 expression in CD4 SP thymocytes (top) and peripheral CD4$^+$ T cells (bottom) from OTII and W131AOTII mice. Data are representative of seven experiments.

Profound developmental defect in TCR tg W131A mice

The increase in memory/effector T cells in the setting of grossly normal T cell development in W131A mice suggested that some compensatory mechanisms, such as a TCR repertoire shift, might mask the previously observed effect of the W131A mutation on TCR signaling. To test this, we introduced the OTII TCR transgene into the W131A background and analyzed the impact of the mutation on positive and negative selection of thymocytes bearing a single TCR specificity. In contrast to W131A mice with a polyclonal TCR repertoire, the number and percentage of CD4SP thymocytes were greatly reduced in W131AOTII mice (Fig. 2, A, top, and B). Moreover, a smaller percentage of Vα2 clonotype-positive CD4SP thymocytes were generated in W131AOTII mice compared with wild-type littermates (Fig. 2 A, bottom). Consistent with a decrease in the CD4SP population, we found that the generation of mature peripheral CD4$^+$ T cells was also impaired in W131AOTII mice (Fig. 2, B and C, top). Most peripheral CD4$^+$ T cells in wild-type littermates exhibited a naive phenotype (CD62L^{high}CD44^{low}), whereas the increased peripheral CD4$^+$ T cells from young adult W131AOTII mice exhibited a phenotype typical of effector/memory cells (CD62L^{low}CD44^{high}; Fig. 2 C, bottom). Moreover, CD69, an early activation marker, was found more frequently on peripheral CD4$^+$ T cells in W131AOTII mice (unpublished data). As the total number of thymocytes and peripheral CD4$^+$ T cells were markedly reduced, it is possible that the abnormal phenotype of peripheral CD4$^+$ T cells from W131AOTII mice resulted from activation by endogenous antigens or by the lymphopenic environment.

Enhanced generation of T reg cells in W131AOTII mice

Despite a lower number of transgene-positive CD4$^+$ T cells in W131AOTII mice, the generation of Foxp3$^+$ T reg cells was substantially increased in the thymus and in the periphery of W131AOTII mice relative to OTII controls (Fig. 2 D). The strength of TCR signaling has been reported to determine the fate of CD4SP thymocytes. Although those CD4SP thymocytes receiving the strongest TCR signal are deleted, thymocytes receiving TCR signals of more moderate strength escape deletion but differentiate into Foxp3$^+$ T reg cells (Josefowicz et al., 2012). Thus, our results suggest that the W131A mutation in Zap70 leads to loss of autoinhibition, leading to stronger TCR-mediated signaling, thereby preferentially favoring the generation of T reg lineage cells. In addition to the T reg cells, we also examined whether the development of other nonconventional αβT cell lineages, such as iNKTs and γδ T cells, might be affected. However, we found no differences in the numbers of iNKT or γδ lineage T cells in the thymus or periphery of W131AOTII mice (unpublished data).

We compared the suppressive abilities of W131AOTII T reg cells with those of OTII T reg cells in vitro. W131AOTII T regs inhibited the proliferation of WT naive cells stimulated with anti-CD3 as efficiently as did OTII T reg cells (unpublished data). Therefore, the T reg cell populations are

substantially expanded in the W131AOTII mice and appear to exhibit normal suppressive function.

Increased apoptosis in DP thymocytes in W131AOTII mice

In light of the enhanced generation of T reg cells in W131AOTII mice, which is suggestive of increased TCR signaling, we investigated the possibility that DP thymocytes from W131AOTII mice might be undergoing negative selection. We first assessed activation-induced cell death in vitro. Thymocytes from either W131OTII or OTII mice were stimulated overnight with medium or plate-bound anti-CD3 plus anti-CD28 in vitro, and expression of Bim, a pro-apoptosis Bcl2 family member, was assessed. The percentages of Bim^+ cells were significantly increased in the stimulated DP thymocytes from W131OTII mice when compared with those from OTII mice (Fig. 3 A). To extend our in vitro findings, we induced apoptosis of thymocytes by i.p. injecting mice with a low dose of anti-CD3 mAb (Kishimoto and Sprent, 1997). Consistent with the in vitro data, fewer viable DP thymocytes from W131AOTII mice were recovered 20 h after anti-CD3 injection compared with DP thymocytes from OTII mice (Fig. 3 B). Collectively, our in vitro and in vivo data strongly argue for an increased sensitivity to TCR-induced apoptosis of W131AOTII DP thymocytes.

To determine whether increased negative selection could account for the reduction of $OTII^+$ CD4SP thymocytes in W131AOTII mice, we crossed W131OTII and OTII mice to a tg line expressing a human Bcl-2 transgene under the control of the proximal lck promoter. As shown in Fig. 3 C, overexpression of the Bcl-2 protein had a minimal effect on promoting the survival of OTII tg^+ CD4SP thymocytes in OTII mice, although we noted an increase in CD8SP thymocytes as was reported previously (Sentman et al., 1991). Interestingly, a more than threefold increase in the number of $OTII^+$ CD4SP thymocytes was observed in W131AOTII mice expressing the Bcl-2 transgene compared with age-matched W131AOTII mice (Fig. 3, C and D). Further analysis of $OTII^+$ CD4SP thymocytes revealed that a greater proportion of CD4SP thymocytes in W131AOTII mice with the Bcl-2 tg expressed CD25 on their surface (Fig. 3 E). Co-staining with Foxp3 antibody showed that the majority of $CD4^+CD25^+$ thymocytes were not T reg cells, suggesting that they were activated but were rescued by overexpression of Bcl-2 (Fig. 3, E–G). Although OTII mice expressing the Bcl-2 tg also showed an elevated percentage of $CD25^+Foxp3^{neg}$ CD4SP thymocytes, the extent of the increase was not nearly as profound as the positive selection in the W131AOTII mice with or without the Bcl-2 transgene (Fig. 3, E and G). Together, we conclude that enhanced negative selection may explain the unexpected decrease in $OTII^+$ CD4SP thymocytes in W131AOTII mice.

The Zap70 W131A mutation results in increased TCR signaling

As increased T reg development and negative selection in W131AOTII mice are predicted to result from stronger TCR signals received by thymocytes during thymic development, we examined whether we could detect altered TCR signaling strength in the context of the restricted OTII TCR repertoire. We took advantage of the Nur77-GFP reporter mouse to study the integrated TCR signal strength perceived by different thymocyte subsets (Zikherman et al., 2012). In line with previous studies (Moran et al., 2011; Zikherman et al., 2012), we found that in OTII mice, the Nur77-eGFP reporter was induced at the time of positive selection, i.e., Nur77 expression was low in preselection DP thymocytes and was up-regulated in postselection DP thymocytes (Fig. 4 A, black line). Interestingly, compared with OTII mice, the Nur77-GFP reporter expression in W131AOTII mice was more markedly increased in postselection DP and CD4SP thymocytes and in a larger proportion of the cells (Fig. 4 A, dashed line). This is suggestive of enhanced TCR signaling and consistent with the putative enhanced negative selection observed in W131OTII mice. As DP thymocytes matured to the CD4SP stage, GFP expression differences diminished but were still apparent between WT and W131A-expressing cells. Likewise, some $OTII^+$, non–T reg cell peripheral T cells exhibited higher GFP expression in the periphery, indicating that a fraction of T lineage cells perceive stronger TCR signals in W131AOTII mice.

To further study Nur77 induction after acute TCR stimulation in vitro, we stimulated thymocytes and $CD4^+$ T cells ex vivo with a combination of anti-CD3 and -CD28 for 3 h and assessed Nur77-GFP expression in DP, CD4SP thymocytes, and peripheral $CD4^+$ T cells (Fig. 4 B). A greater proportion of DP and CD4 SP thymocytes isolated from W131AOTII mice up-regulated Nur77 expression and did so to a greater extent more than did thymocytes from OTII mice. Collectively, our findings suggested that W131AOTII thymocytes and peripheral $CD4^+$ T cells exhibited enhanced basal TCR signaling compared with OTII thymocytes and further up-regulated Nur77-GFP in response to TCR stimulation.

Defective IL-2 production in W131AOTII mice and hyporesponsiveness

Because Nur77 GFP expression reflects integrated TCR downstream signaling over time (Au-Yeung et al., 2014), we next investigated whether other TCR-dependent events were enhanced in the peripheral T cells from W131AOTII mice. We measured IL-2 production and induction of activation markers, such as CD25 and CD69, as indicators of productive T cell activation. Sorted non–T reg cell and naive $CD4^+$ T cells from OTII, $Zap70^{+/-}$OTII (to control for lower Zap70 expression), or two W131AOTII mice were cultured in vitro for 16 h with APCs loaded with OVA 323–339 peptide. As expected, a substantial proportion of naive $CD4^+$ T cells from both OTII and $Zap70^{+/-}$OTII mice secreted IL-2 after stimulation (Fig. 5 A). Additionally, both CD25 and CD69 were markedly up-regulated in these cells (Fig. 5, B and C). In contrast, the proportion of IL-2–secreting $CD4^+$ T cells from W131AOTII mice was greatly

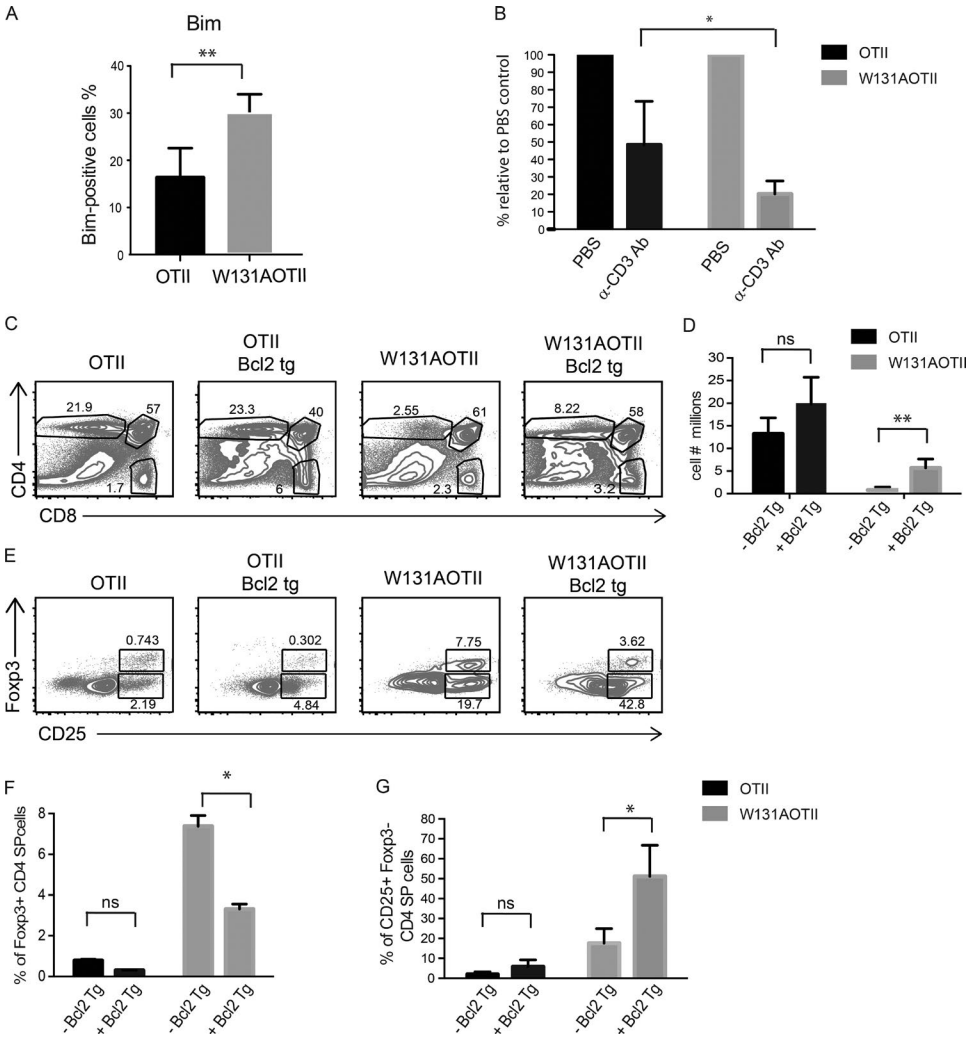

Figure 3. **Evidence for enhanced negative selection in W131AOTII mice.** (A) In vitro–induced apoptosis of OTII or W131AOTII DP thymocytes, analyzed by intracellular staining of Bim after 16 h of incubation in plate-bound anti-CD3 and anti-CD28. (B) In vivo injection of anti-CD3 to mimic negative selection. Age-matched OTII and W131AOTII mice were injected i.p. with 10 µg/ml of either PBS or anti-CD3 mAb. After 20 h, cell numbers of DP thymocytes were determined and were compared with animals injected with PBS. Data are pooled from two independent experiments with four mice per genotype. (C and E) Flow cytometry of thymocytes from thymi of OTII and W131AOTII mice with or without the lck-bcl2 transgene. (C) Representative plot showing CD4/CD8 profile of freshly isolated thymocytes from the indicated genotypes. (D) Quantification of absolute CD4SP cell counts from OTII and W131AOTII with or without lck-bcl2 transgene. $n = 5$ per genotype. (E) Expression of Foxp3 versus CD25 of CD4SP thymocytes from the indicated genotypes. Data shown are representative of three independent experiments. (F) Percentages of $Foxp3^+CD4SP$ thymocytes from the indicated genotypes. (G) Percentages of $CD25^+Foxp3^{neg}$ CD4SP thymocytes from the indicated genotypes. $n = 5$ per genotype. All error bars represent SEM. NS, not significant; *, $P < 0.05$; **, $P < 0.01$.

reduced as were the induction of CD25 and CD69 after antigen stimulation (Fig. 5).

To assess whether T cell hyporesponsiveness in W131AOTII $CD4^+$ T cell also occurs in vivo, we co-transferred fluorescent dye–labeled OTII and W131AOTII $CD4^+$ T cells at a ratio of 1:1 into congenic hosts that were then immunized in the footpad with OVA protein. In vivo proliferative responses were measured by dye dilution. At 72 h after immunization, we found that OTII $CD4^+$ T cells underwent robust proliferation, whereas W131AOTII $CD4^+$ T cells proliferated less to OVA protein (Fig. 5, D and E). Together, our data revealed a cell-intrinsic impaired response of the peripheral $CD4^+$ T cells from W131AOTII mice to antigen, which contrasts with their higher TCR basal signaling detected by Nur77-GFP expression.

$CD4^+$ T cells from W131AOTII mice displayed an anergic phenotype

The diminished responses of $CD4^+$ T cells from W131AOTII mice led us to hypothesize that these peripheral $CD4^+$ T cells might be anergic. We found the transcript levels of GRAIL, an E3 ubiquitin ligase implicated in anergy (Heissmeyer and Rao, 2004), from $CD4^+$ T cells of W131AOTII mice were increased by 4–5-fold compared with those of the control $CD4^+$

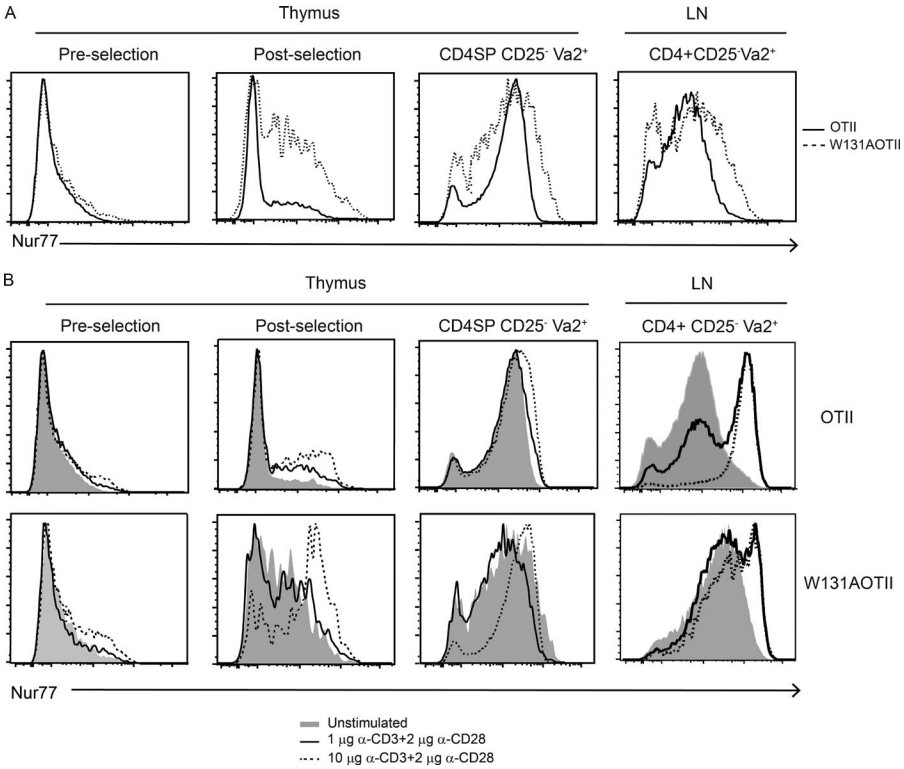

Figure 4. **Evidence for enhanced TCR signaling in W131AOTII mice.** (A) Assessment of Nur77-GFP fluorescence in freshly isolated thymic subsets or T cells from OTII and W131AOTII harboring the Nur77-GFP reporter. DP thymocytes were further subdivided into preselection ($CD5^{int}$ $TCR\beta^{int}$) and post-selection ($CD5^{hi}TCR\beta^{hi}$) stages based on CD5 and TCR expression (B) Thymocytes or peripheral $CD4^+$ T cells from OTII and W131AOTII harboring the Nur77-GFP reporter were stimulated with plate-bound anti-CD3 and anti-CD28 for 3 h, and then analyzed by flow cytometry to assess Nur77-GFP fluorescence in preselection and post-selection DP and CD4SPCD25-V$\alpha2^+$ thymocytes and $CD4^+$CD25-$Va2^+$ T cells. Data shown are representative of three experiments.

T cells (Fig. 6 A). Similarly, the expression of the Egr2 protein, implicated in T cell anergy (Safford et al., 2005), was elevated in W131AOTII cells (Fig. 6 B). Moreover, a recent study has shown that coexpression of CD73 and folate receptor 4 (FR4) defines a population of naturally occurring anergic T cells (Kalekar et al., 2016). This prompted us to investigate whether the $CD73^{hi}FR4^{hi}$ anergic population might be increased in W131AOTII mice. Indeed, in both naive $Foxp3^{neg}CD44^{lo}$ and activated $Foxp3^{neg}CD44^{hi}$ CD4 T cells, we observed an increase in the $CD73^{hi}FR4^{hi}$ anergic population in W131AOTII mice compared with OTII mice (Fig. 6 C, top and bottom). Together, these results suggest that $CD4^+$ T cells from W131AOTII mice may be diverted to an anergic state.

Striking up-regulation of inhibitory receptors in W131AOTII T cells

To reconcile the increased TCR signal strength observed in the thymus and the anergic-like phenotype in the periphery, we examined the surface expression of several inhibitory receptors, which have been shown to dampen downstream TCR signaling and cause T cell unresponsiveness (Rodriguez-Manzanet et al., 2009; Odorizzi and Wherry, 2012). In OTII thymocytes, PD-1 expression is low at the DP stage (unpublished data). In contrast, we were able to readily detect PD-1 expression on post-positive selection DP thymocytes in W131AOTII mice (Fig. 6 D, top). More strikingly, PD-1 expression was further up-regulated on CD4SP thymocytes from W131AOTII mice (Fig. 6 D, top). Whereas PD-1 expression was hardly detectable in OTII peripheral $CD4^+$T cells, PD-1 expression was elevated on a substantial subset of the peripheral $CD4^+$ T cells in W131AOTII mice, particularly of the memory/effector subset (Fig. 6 D, top). Similar to PD-1, we also found that the expression of another inhibitory receptor, Tim-3 (Fig. 6 D, bottom), was up-regulated on W131AOTII thymocytes and peripheral T cells (Fig. 6 D, bottom). Of note, we found that T cells isolated from W131A mice with a polyclonal TCR repertoire also expressed higher levels of PD-1 compared with T cells from wild-type controls (unpublished data). Among other known inhibitory receptors that we screened, CTLA-4, LAG3, and TIGIT were not up-regulated on W131AOTII T cells (unpublished data). Interestingly, we also found that the majority of the $CD73^{hi}FR4^{hi}$ anergic population in W131AOTII mice was contained in the $PD\text{-}1^+$ T cell subset, whereas $PD\text{-}1^-$ T cells exhibited very little enrichment of this population (Fig. 7 E). This was consistent with the previous study that found that PD-1 was one of the genes that was enriched in the $CD73^{hi}FR4^{hi}$ anergic T cell population (Kalekar et al., 2016). Overall, these data suggest that several negative regulatory mechanisms, including the expression inhibitory receptors, are induced in response to enhanced TCR signaling in W131AOTII mice.

The increase in T reg cells and up-regulation of PD-1 on W131AOTII $CD4^+$ T cells are cell intrinsic

To address whether the increase in the T reg cell population and increase in $PD\text{-}1^+$ cells in W131AOTII mice were cell-intrinsic or a consequence of the lymphopenic environment, we generated mixed bone marrow chimeras in which OTII and W131AOTII bone marrow cells with different congenic

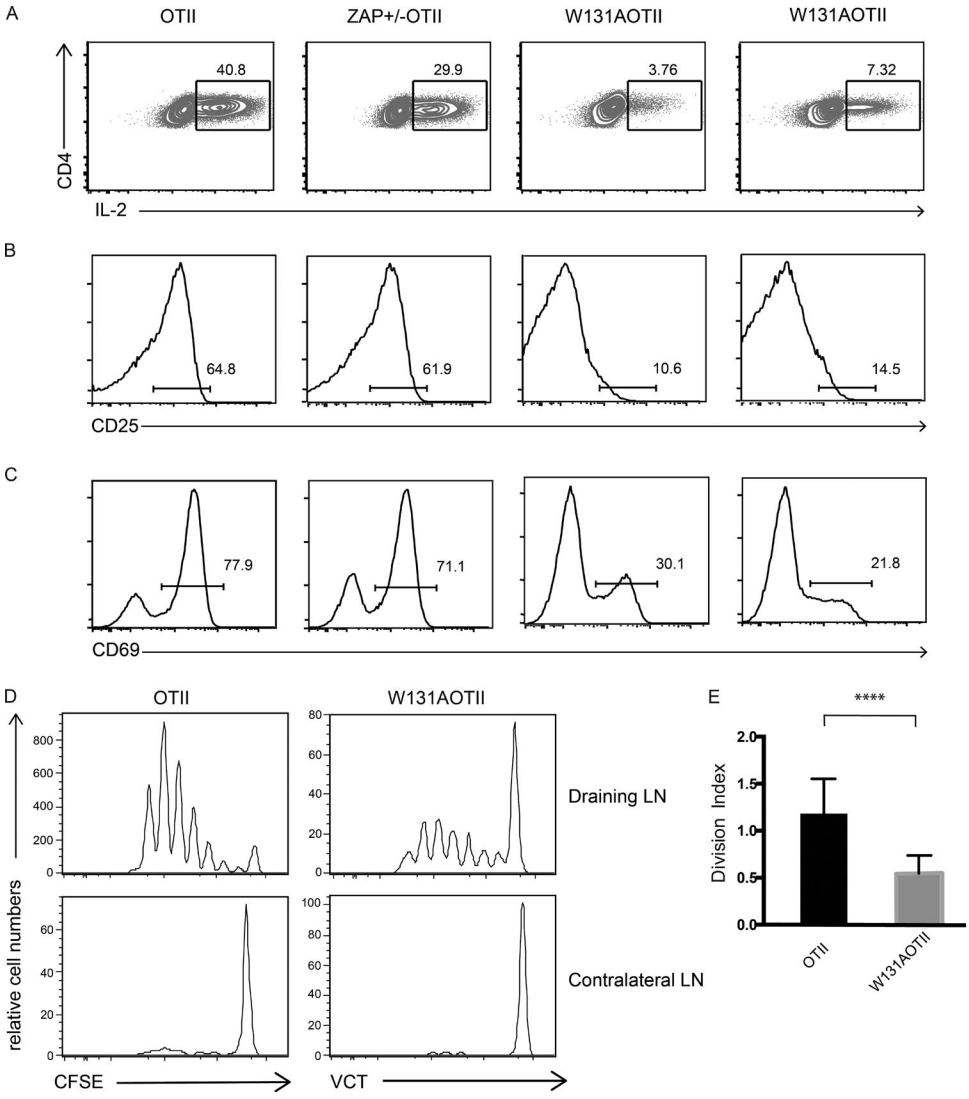

Figure 5. **Peripheral CD4$^+$ T cells from W131AOTII mice are hyporesponsive to antigen challenge.** Naive CD4$^+$ T cells from W131OTII mice exhibit impaired IL-2 production (A) and defective up-regulationof CD25 (B) and CD69 (C). (A–C) Sorted naive CD4$^+$ T cells from age-matched OTII, Zap70$^{+/-}$OTII, and two W131AOTII mice were cultured in vitro with splenocytes from TCR$\alpha^{-/-}$ mice and 1 µM OVA peptide for 16 h. Cells were subsequently stained for the indicated activation markers or secreted IL-2. Results are representative of two independent experiments with two to three mice for each genotype. (D) Proliferative responses of OTII and W131AOTII CD4$^+$ T cells after antigen challenge in vivo. CD4$^+$CD25$^-$ T cells from OTII and W131AOTII mice were loaded with CFSE and violet cell trace (VCT) dyes, respectively. Cells, mixed at a 1:1 ratio, were adoptively transferred into CD45.1$^+$ congenic hosts. Host mice were immunized the next day with 25 µg OVA protein in complete Freund's adjuvant. Dilution of cell trace dyes was measured by flow cytometry 3 d after immunization. Results are representative of three independent experiments with nine mice in each genotype. (E) Division index of in vivo proliferative response from draining LN cells. All error bars represent SEM. ****, $P < 0.0001$.

markers were transferred at a 1:1 ratio into lethally irradiated hosts. As shown in Fig. 7 A, we observed approximately equal representation of OTII and W131AOTII thymocytes at the DN and DP stages. In striking contrast, significantly fewer CD4SP thymocytes and peripheral CD4$^+$CD25$^-$ T cells were generated from W131AOTII bone marrow cells than from OTII mice (Fig. 7 A). This finding is consistent with the developmental defect seen in the intact W131OTII mice (Fig. 2 C), suggesting that the defective generation of CD4SP thymocytes and CD4$^+$ T cells in the periphery in W131AOTII mice is cell intrinsic. Despite W131AOTII CD4 T cells having a developmental disadvantage in the periphery, in contrast to the OTII T cells, the enhanced generation of T reg cell population and the up-regulation of PD-1 were still seen on the W131AOTII T cells in the chimeric mice (Fig. 7, B and C). Together, these data suggest that these phenotypes are likely caused by enhanced cell-intrinsic TCR signaling in W131OTII mice rather than the lymphopenic environment.

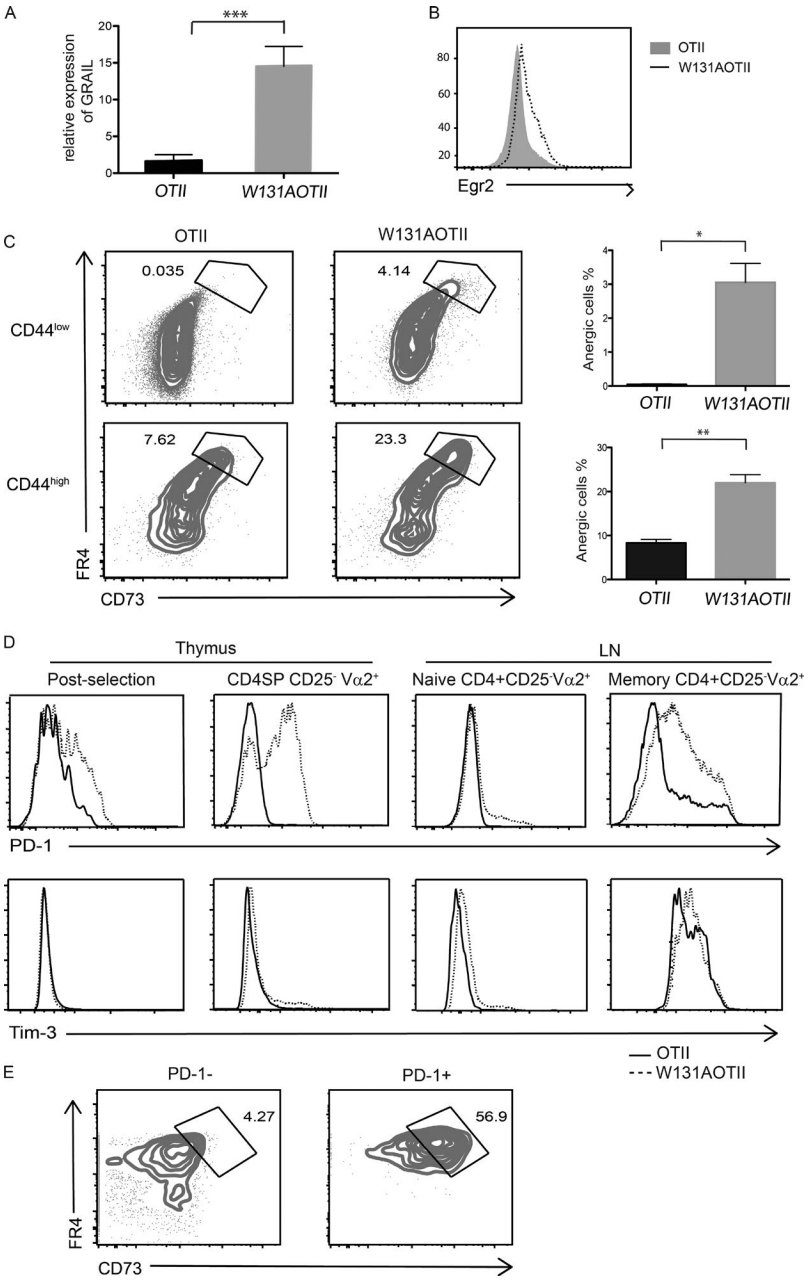

Figure 6. **Peripheral CD4$^+$ T cells from W131AOTII mice display an anergic phenotype.** (A) Increased mRNA expression of GRAIL in naive CD4$^+$OTII$^+$ peripheral T cells from W131AOTII mice. Data are pooled from two independent experiments (n = 4 per genotype). (B) Increased expression of the Erg2 transcription factor in naive CD4$^+$OTII$^+$ peripheral T cells from W131AOTII mice. Results are representative of two independent experiments with three mice in each genotype. (C) CD44^{low} (naive, top) and CD44^{high} (memory/activated, bottom) splenocytes from either 2-mo-old OTII or W131AOTII mice were stained for CD73 and FR4 on CD4$^+$ Foxp3^{neg} T cells. Percentages in CD73^{hi}FR4^{hi} gate are shown. Results are quantified (right) for CD44^{low} (top) and CD44^{high} (bottom) cells of the indicated genotypes. (D) Flow cytometric analysis of expression of indicated inhibitory receptors at various stages of thymic development and naive or memory LN T cells. Data shown are representative of four independent experiments. (E) Comparison of frequency of CD4$^+$Foxp3^{neg}CD44^{hi}CD73^{hi}FR4^{hi} T cells in PD-1$^+$ and PD-1$^-$ populations from W131AOTII splenocytes. Data are pooled from 2 independent experiments with four mice per genotype. All error bars represent SEM. *, $P < 0.05$; **, $P < 0.01$; ***, $P < 0.001$.

Higher basal TCR signaling but diminished inducible signaling in W131AOTII T cells

Previous studies have shown that PD-1 exerts its inhibitory function by antagonizing TCR downstream signaling (Sheppard et al., 2004; Yokosuka et al., 2012). To examine the effect of up-regulation of inhibitory receptors upon TCR signaling, we assayed TCR-induced calcium increases and ERK phosphorylation in cells from these mice (Fig. 8). Unlike the W131A mutant in Jurkat cells, which exhibited hyperresponsiveness to TCR simulation (Deindl et al., 2009), CD4SP thymocytes from W131AOTII mice displayed lower calcium increases in response to anti-CD3 cross-linking. The TCR-induced calcium response was even further reduced in peripheral CD4$^+$ naive and memory T cells from W131AOTII mice (Fig. 8 A). We also observed slightly lower anti-CD3–induced ERK phosphorylation in W131AOTII DP and CD4SP thymocytes compared with OTII thymocytes (Fig. 8 B). In contrast, in peripheral CD4$^+$ T cells, ERK phosphorylation in response to anti-CD3 was markedly reduced from W131AOTII T cells when compared with OTII thymocytes (Fig. 8 C, top). Interestingly, although TCR-induced responses were greatly diminished in W131AOTII CD4$^+$ T cells, both free cytoplasmic calcium concentrations and Erk phosphorylation were reproducibly elevated in the resting,

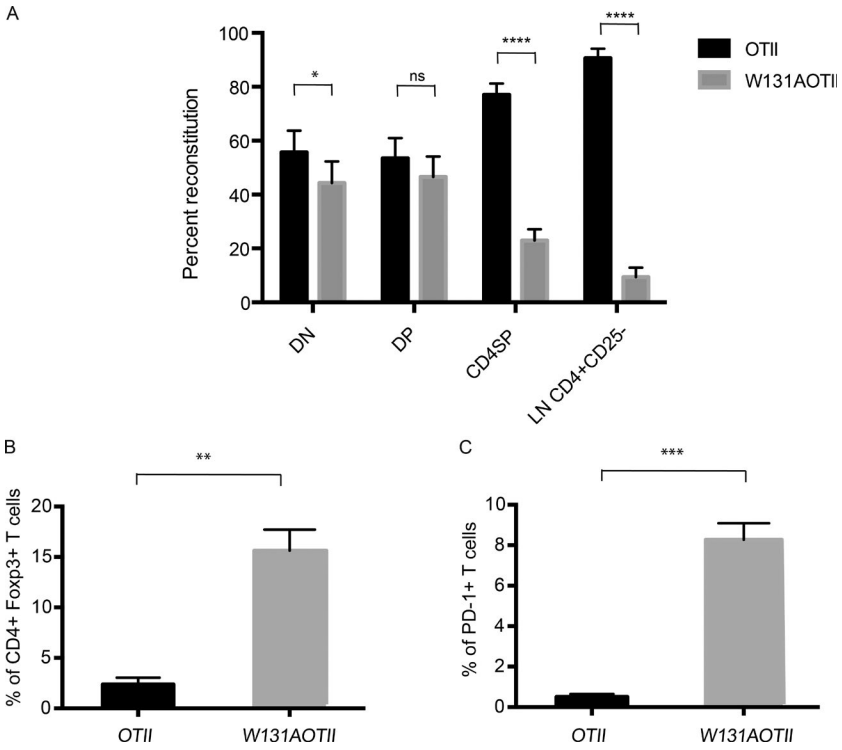

Figure 7. **Increase in T reg cells and elevated PD-1 expression in W131AOTII CD4$^+$ T cells are cell intrinsic.** (A) Competitive repopulation of OTII and W131AOTII donor bone marrow cells, injected at a 1:1 ratio, was assessed in mixed bone marrow chimera 8 wk later. (B) Percentages of peripheral T reg cells (Foxp3$^+$) generated from mixed bone marrow chimeras. (C) Percentages of PD-1$^+$ CD4 T cells generated from mixed bone marrow chimeras. Data are representative of two independent experiments with six chimeras. All error bars represent SEM. **, $P < 0.01$; ***, $P < 0.001$.

basal state (Fig. 8 A, left, C, bottom, and D). Others have reported an effect of PD-1 in down-regulating the TCR-induced AKT–mTOR pathway (Wherry and Kurachi, 2015). We examined TCR-induced activation of the AKT–mTOR pathway by assessing phosphorylation of AKT kinase and the direct mTORC1 substrate ribosomal protein S6 kinase in peripheral CD4$^+$ T cells. Indeed, we found that the activation of the AKT/mTOR pathway appears to be attenuated in W131AOTII CD4$^+$ T cells after stimulation by anti-CD3, as indicated by the reduced amounts of phospho-AKT and S6 kinases (Fig. 8 E, top and bottom). Moreover, reduced levels of AKT and S6 phosphorylation were also observed in the peripheral CD4$^+$ from W131A mice with a polyclonal TCR repertoire (unpublished data). Collectively, our findings suggest that up-regulation of inhibitory receptors in W131A T cells correlates with higher basal signaling and a negative impact on several TCR-induced signaling pathways.

Anti–PD-1 treatment partially reverses T cell unresponsiveness in W131AOTII mice

To determine whether up-regulated inhibitory receptors such as PD-1 could account for T cell unresponsiveness in the periphery of W131AOTII mice, we treated OTII and W131AOTII mice with anti–PD-1 mAb. We i.p. injected either anti–PD-1 mAb (J43) or control IgG (hamster IgG) into mice three times a week for 3 wk, beginning at 4 wk of age. As shown in Fig. 9, we found no substantial difference in IL-2 production, or induction of activation markers comparing OTII mice treated with either control IgG or anti–PD-1 mAb. In contrast, anti–PD-1 mAb treatment in W131AOTII mice partially reversed T cell unresponsiveness as detected by increased IL-2 production and greater induction of CD25 and CD69 after TCR stimulation. Together, we conclude that the PD-1 inhibitory pathway contributes to T cell hyporesponsiveness in W131AOTII mice.

DISCUSSION

In the present study, we characterized a mouse model to evaluate whether altering Zap70 regulation by impairing its autoinhibition impacts T cell development or T cell function. The W131A mutation partially disrupts the autoinhibition of the Zap70 kinase. More specifically, this mutation bypasses the first step in relieving autoinhibition, a role played by phospho-ITAM binding. However, we failed to detect changes in thymocyte development and only had subtle hints of perturbed T cell function (i.e., more effector/memory and T reg cells) in W131A mice with a diverse TCR repertoire. In the context of the OTII tg system, where compensation to increased TCR signaling via repertoire shift was not possible, enhanced TCR signaling strength, a result of the W131A mutation, was clearly revealed. Higher TCR signaling strength in W131AOTII mice was manifested most clearly by increased expression of Nur77 in CD4 thymocytes and peripheral CD4$^+$ T cells. With a fixed repertoire, this increased signaling perturbed thymocyte development, increasing the number of cells diverted to the T reg lineage or undergoing negative selection. Therefore, our results emphasize the importance of tight control of Zap70 kinase activity and TCR signaling during T cell development. Increased signaling from cells with the W131A mutation in Zap70 led to additional

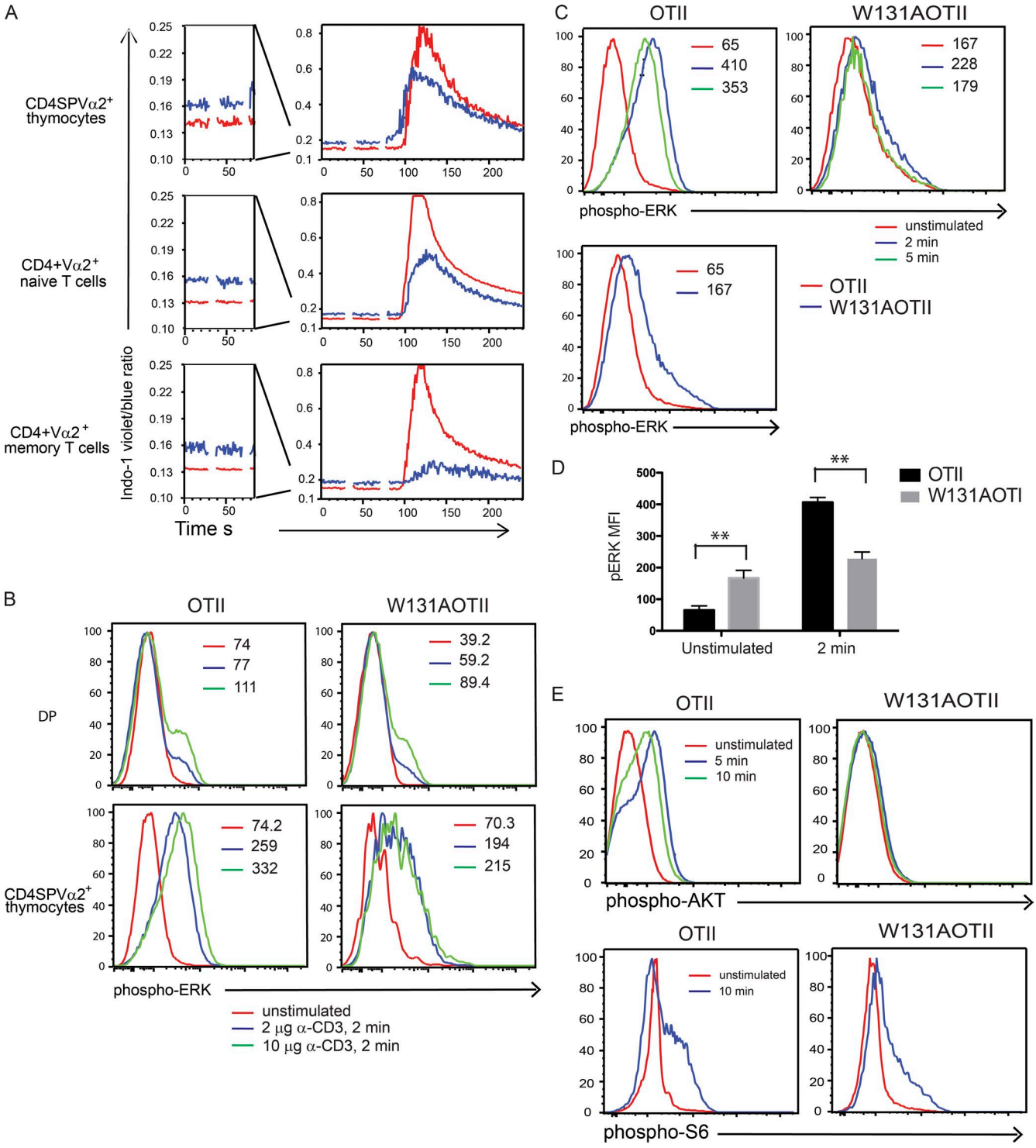

Figure 8. **The W131A mutation results in increased basal signaling but diminished TCR-induced signaling.** (A) Calcium responses of thymocytes and peripheral T cells in OTII and W131AOTII mice. Thymocytes or purified CD4+ T cells from both genotypes were first stained with anti-CD45 with different fluorochrome conjugates, mixed together, and loaded with Indo-1 to detect intracellular calcium. Cells were stimulated with 10 μg/ml anti-CD3, followed by cross-linking with 50 ng/ml anti–Armenian hamster IgG. (left) Basal calcium responses. Red and blue lines indicate OTII and W131AOTII, respectively. (B–D) Flow-based assessment of ERK phosphorylation. Thymocytes (B) or purified peripheral CD4+ T cells (C) were stimulated with anti-CD3 cross-linking for the indicated times. (C) Erk phosphorylation in peripheral CD4+ T cells was shown over time after stimulation (top). Overlay depicts one representative experiment of basal Erk phosphorylation between OTII and W131AOTII CD4+T cells (bottom). (D) Quantification of mean fluorescence (MFI) of ERK phosphorylation

compensatory mechanisms within thymocytes and peripheral T cells that was manifested by up-regulation of inhibitory pathways that led to T cell hyporesponsiveness. Together, by altering TCR signaling, multiple levels of immune tolerance mechanisms were engaged.

In our previous cell line studies, Zap70-deficient Jurkat cells reconstituted with the W131A mutant exhibited hyperresponsiveness, such as increased TCR-induced calcium responses and enhanced phosphorylation of LAT, PLCγ1, and ERK (Deindl et al., 2009). Unlike these cell line studies, no obvious signaling defects downstream of TCR were observed in the T cells from W131A mice with the polyclonal TCR repertoire. The difference in these results between Jurkat cells and T cells may reflect plasticity in the mouse cells to engage various levels of regulatory mechanisms, apparently not possible in Jurkat cells. One example is the likely repertoire shift that occurred in early thymocyte development manifested in cells with a diverse TCR repertoire. Although the compensatory mechanisms in mice resulted in relatively normal T cell development in W131A mice with a polyclonal repertoire, increased generation of the T reg cell population and of memory $CD4^+$ T cells provides some evidence for enhanced TCR signaling. When the ability to compensate for increased TCR signaling via repertoire shift was eliminated by fixing the TCR repertoire, the majority of immature W131AOTII thymocytes with hyperresponsive TCR signaling were either deleted through negative selection or differentiated into the T reg cell lineage. In support of this notion, when the Bcl-2 transgene was introduced into either OTII or W131AOTII mice, a greater proportion of $Foxp3^{neg}CD4SP$ thymocytes expressing high levels of CD25 were rescued in W131AOT II mice as compared with OTII mice (Fig. 3). Additionally, W131AOTII DP thymocytes manifested a greater increase in Nur77 GFP induction than did OTII thymocytes in the basal state and when stimulated in vitro with anti-CD3 and anti-CD28 (Fig. 4). Together, these findings suggest that by fixing the TCR repertoire enhanced TCR signaling becomes evident during thymic selection.

As thymocytes matured, another negative feedback mechanism for increased TCR signaling was engaged and manifested in the W131A mice. Inhibitory receptors, such as PD-1 and Tim-3 that functionally down-regulate TCR-mediated pathways that were increased in the CD4SP thymocytes of W131AOTII mice. PD-1 is primarily expressed on DN αβ and γδ T cells in the thymus (Okazaki et al., 2013). Its expression is rapidly down-regulated once thymocytes complete β-selection and mature to the DP stage. The striking up-regulation of PD-1 at the CD4SP stage led us to postulate that these inhibitory receptors play a role in down-modulating TCR signaling in more mature W131AOTII thymocytes. Indeed, we provided evidence that the calcium, Erk, and AKT–mTOR pathways are attenuated in W131AOTII thymocytes after TCR stimulation. These results suggested that enhanced PD-1 expression in W131AOTII mice may modulate TCR signaling threshold in the thymus.

The role of PD-1 expression in the thymus has not been characterized as extensively as its role in the periphery. A previous study also demonstrated that PD-1 overexpression in the thymus inhibits positive selection in the HY TCR tg model by impairing thymocyte maturation, including CD69 up-regulation (Keir et al., 2005). Interestingly, we began to observe up-regulation of PD-1 in post-selection ($CD5^{high}$ $TCR\beta^{high}$) DP thymocytes in W131AOTII mice. It is possible that enhanced PD-1 expression has a negative impact on positive selection, thereby explaining the marked reduction of $OTII^+$ CD4SP thymocytes in W131AOTII mice, in addition to the enhanced negative selection observed.

The impact of the increased TCR signaling resulting from the W131A mutation, leading to expression of inhibitory receptor signaling, was also manifested in mature naive and memory peripheral T cells. Notably, W131AOTII $CD4^+$ T cells showed a greater reduction in TCR signaling than did W131AOTII thymocytes. One possibility could be the intrinsic difference between peripheral $CD4^+$ T cells and thymocytes in their sensitivity to inhibitory receptor-mediated regulation. The other possibility is that anergy-associated proteins, such as GRAIL (Whiting et al., 2011) and Egr2 (Safford et al., 2005) were up-regulated in peripheral $CD4^+$ T cells. Thus, in addition to expression of the inhibitory receptors, additional down-modulation of TCR signaling was further enforced by increased expression of GRAIL and Egr2, resulting in dampened inducible signaling in W131AOTII $CD4^+$ T cells. In support of this, we found that anti–PD-1 mAb treatment only partially restored IL-2 production, suggesting that the hyporesponsiveness in W131AOTII $CD4^+$ T cells resulted from multiple mechanisms and may involve integration of several negative regulatory pathways throughout T cell development and in the periphery.

Whereas inducible TCR signaling in W131AOTII $CD4^+$ T cells was greatly impaired, basal cytoplasmic free calcium and ERK phosphorylation were elevated. This is reminiscent of anergic B cells reported in the HEL- and Ars-specific BCR tg model systems (Cambier et al., 2007). In both BCR tg systems, high basal signaling is thought to result from chronically occupied BCR on anergic B cells. It is possible that, similar to anergic B cells, TCRs from W131AOTII T cells with hyperactive Zap70 kinase are activated by chronic interaction with endogenous antigens.

levels from the indicated genotypes is shown, illustrating higher basal ERK levels in W131AOTII T cells, compared with OTII T cells. $n = 5$ per genotype. All error bars represent SEM. **, $P < 0.01$. (E) Flow-based assessment of AKT (top) and S6 (bottom) phosphorylation. Purified $CD4^+$ T cells from OTII and W131AOT II mice were stimulated with anti-CD3 cross-linking for 10 min. Phosphorylated-AKT and -S6 were assessed by intracellular staining. Data are representative of at least three independent experiments.

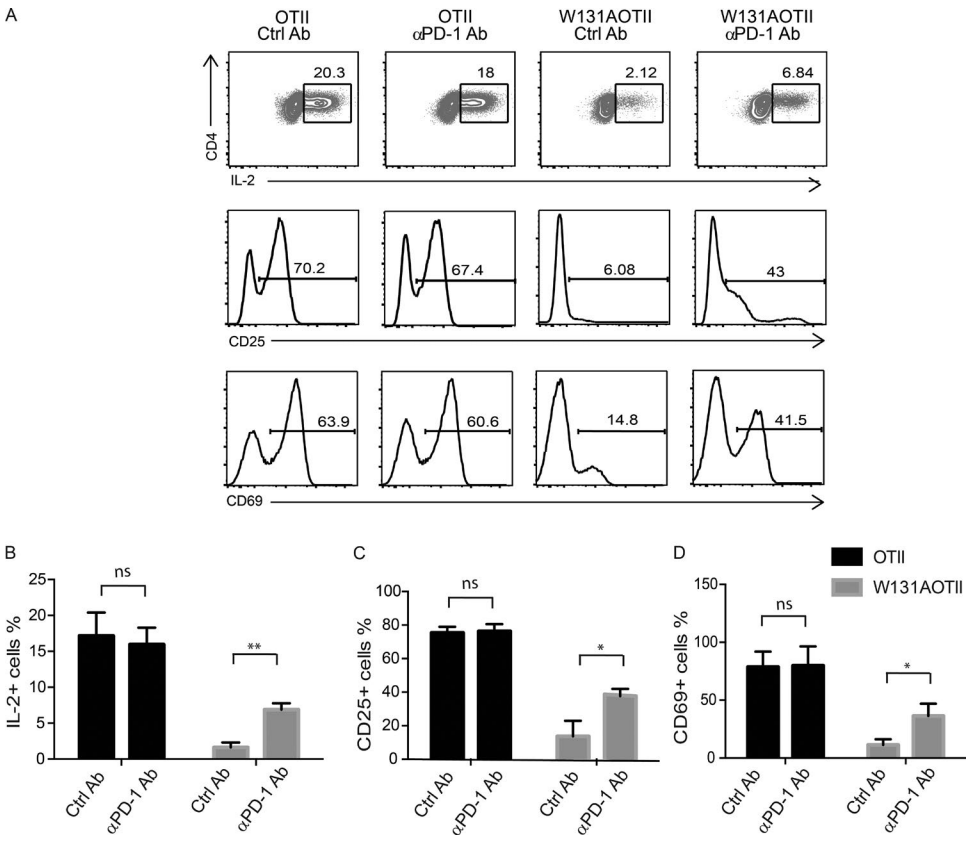

Figure 9. **Anti–PD-1 mAb treatment partially reverses T cell unresponsiveness in W131AOTII mice.** Anti–PD-1 mAb or control IgG were administrated i.p. to 4-wk-old OTII or W131AOTII mice every other day for 3 wk to determine the role of PD-1 during anergy induction. Responses of naive $CD4^+$ T cells were assessed by IL-2 production (top) and up-regulation of CD25 (middle) and CD69 (bottom) and. Data are representative of two independent experiments ($n \geq 4$ per group). (B–D) Graphs depict the quantification of the results from A. Percentages of $Il\text{-}2^+$ (B), $CD25^+$ (C), and $CD69^+$ (D) cells are shown. All error bars represent SEM. NS, not significant; *, $P < 0.05$; **, $P < 0.01$.

In support of this, we observed higher GFP expression in W131AOTII T cells throughout thymocyte development and in the periphery, even though the cognate OVA antigen was not expressed (Fig. 4 A). Together, these data suggest continuous recognition of some self-peptide-MHC class II in W131AOTII T cells contributes to the phenotypes observed in the W131AOTII mice.

Our characterization of peripheral T cells in W131AOTII mice reveals many features that resemble other hyporesponsive states in T cells such as anergy (Mueller and Jenkins, 1995; Schwartz, 2003) and exhaustion (Wherry and Kurachi, 2015). For instance, the finding that W131AOTII $CD4^+$ T cells failed to produce IL-2 efficiently or up-regulate CD69 and CD25 after OVA peptide stimulation was very similar to what has been seen in anergic T cells that are triggered by their TCRs without an adequate co-stimulatory signal through CD28. Furthermore, several negative regulatory molecules involved in anergy induction, such as GRAIL and Egr2, were also up-regulated in W131AOTII $CD4^+$ T cells. However, unlike clonal anergy resulting from incomplete T cell stimulation, no substantial differences were found on the surface expression of CD28 and CTLA-4 between OTII and W131AOTII mice (unpublished data). Alternatively, increased expression of inhibitory receptors observed in W131AOTII T cells is commonly seen in T cell exhaustion that often occurs in chronic viral infection and cancers (Crespo et al., 2013; Pauken and Wherry, 2015). Exhausted T cells in these settings progressively lose their ability to produce effector cytokines and retain their cytotoxic potential. Similarly, in W131AOTII mice, up-regulation of inhibitory receptors was first identified in the thymus, but T cell dysfunction became most obvious in the peripheral $CD4^+$ T cells. It is possible that the negative regulatory mechanisms operative in T cell anergy and exhaustion may all contribute toward the T cell hyporesponsiveness observed in W131AOTII mice.

Recently, it has been reported that $CD4^+$ T cells undergoing clonal anergy induce high-level expression of CD73 and FR4 (Kalekar et al., 2016). That study suggested that $CD73^{hi}FR4^{hi}$ anergic T cells have the potential to become T reg cells in a lymphopenic environment. This conversion was suggested to be important for the avoidance of autoimmunity, as removal of anergy-derived T reg cells results in the

development of autoimmunity. Similarly, we demonstrated a greater frequency of $CD73^{hi}FR4^{hi}$ anergic T cell population in antigen-experienced CD44 "high" non-T reg cells in W131AOTII mice as compared with OTII mice. Interestingly, the $CD73^{hi}FR4^{hi}$ anergic T cell population corresponds to T cells with increased PD-1 expression. Although the roles of CD73 and FR4 in induction or maintenance of anergy process remain unclear, up-regulation of these two molecules in W131AOTII T cells supports the notion that W131OTII T cells acquire an anergic state in response to increased TCR signaling.

Unlike the anergic phenotype observed in W131AOTII mice described here, in a recent study, a combination of hypomorphic and autoinhibitory destabilizing mutations of ZAP70 in two affected children in a family led to early onset of several profound manifestations of autoimmunity (Chan et al., 2016). Although the difference between our mouse model and these patients could be due to the differences in the impacts of each of the constitutively active ZAP70 mutations, it is likely that other genetic modifiers may also contribute to disease manifestations superimposed on the hypermorphic allele of ZAP70. In line with that, genome-wide association studies have uncovered many genetic loci associated with autoimmune diseases (Hardy and Singleton, 2009). Each locus exerts a small effect on disease risk; however, combinations of genetic variants confer a graded risk of disease. The C57BL/6 mouse background into which the W131A mutation was introduced may not have a sufficient predisposition for autoimmunity. In contrast, the patients described by Chan et al. (2016), may have other genetic modifier loci that predispose them for autoimmunity in the setting of increased ZAP70 activity. Moreover, recent identical twin studies highlighted the importance of environmental factors as key determinants of human autoimmune phenotypes (Imboden, 2009). Therefore, it is possible that W131AOTII mice reared in a specific pathogen–free facility lack the exposure to a variety of microbes that could influence the development of autoimmune diseases.

In summary, our findings provide some new insights into how inhibitory receptors function as rheostats that restrain inappropriate activation of TCR signaling throughout T cell development and link both central and peripheral tolerance mechanisms to keep potentially autoreactive T cells or T cells with inappropriately high TCR signaling in check. Our W131A mice may prove to be a useful genetic model to understand the complex inhibitory pathways that can impair or control T cell responses.

MATERIALS AND METHODS

Generation of *Zap70* W131A mice

Zap70 W131A knock-in mice were generated by a gene targeting strategy. 1.7 kb of a 5′ homologous arm and 1.2 kb of a 3′ homologous arm were generated by PCR from C57BL/6 mouse genomic DNA. The 5′ homologous arm containing murine *zap70* exon 2 and 3 was subjected to site-directed mutagenesis changing tryptophan 131 to alanine and simultaneously introducing a diagnostic Hind III site. The mutated 5′ homologous arm and 3′ homologous arm was subcloned into a targeting vector containing Neo cassette floxed by the loxP sequence. The final targeting construct was confirmed by sequencing. Linearized DNA was electroporated into C57BL/6-derived embryonic stem (ES) cells (gift from A. Ma, University of California, San Francisco, San Francisco, CA). Homologous recombinants were selected in the presence of G418. DNA from each ES colony was first screened by genomic PCR using primers covering the neo gene and the 5′ homologous arm (Fig. 1 A, magenta arrowheads). Genomic DNA from potential ES clones was digested with EcoRI and analyzed by Southern blotting using the 5′ external probes shown in Fig. 1 A. Two positive clones with correctly targeted alleles and knock-in mutations were also confirmed by sequencing and injected into C57BL/6 blastocysts. Chimeric mice were generated and mated with C57BL/6 females for germline transmission. The *neo* gene was further excised by crossing mutant mice to E2a Cre-tg mice obtained from The Jackson Laboratory. Excision of the *neo* gene was confirmed by genomic PCR. E2a cre-tg from the positive mutant mice was removed by crossing several generations with C57BL/6 mice. Mice with the W131A allele and no cre-tg were intercrossed to obtain homozygous W131 mutant mice. The primers used for screening are as follows: 5′ primer, 5′-CATGACCTGGAAGGAGGACTTG-3′; 3′ primer, 5′-TGGAGGAACCTCTGTCAGCTCTAAG-3′. The size of the PCR product is 305 bp for the wild-type allele and 530 bp for the W131A allele.

Mice

All mice were bred and maintained in a specific pathogen–free facility and all studies were done according to the Institutional Animal Care and Use Committee guidelines of the University of California (San Francisco, CA). Lck-Bcl2 and Nur77-eGFP tg mice were described previously (Sentman et al., 1991; Zikherman et al., 2012). WT C57BL/6 OTII TCR tg mice were purchased from The Jackson Laboratory. $Zap70^{+/-}$OTII and W131AOTII mice were generated in our laboratory by crossing OTII mice with $Zap70^{-/-}$ or W131A mice, respectively.

Antibodies

The following antibodies were used for staining: CD4 PerCp-Cy5.5, TCRβ PerCp-Cy5.5, and CD62L APC (TONBO); CD44 FITC, PD-1 (29F.1A12) PE-Cy7, CD69 PE-Cy7, CD5 PerCp-Cy5.5, CD8α Pacific Blue, and TCRβ Pacific Blue (BioLegend); CD44 PE-Cy7, CD8α (APC-eFluor 780), CD4 Qdot606, and Zap70 FITC (Life Technology). In vivo anti-PD (J43) antibody and control IgG were purchased from BioXcell. For intracellular flow cytometry, antibodies against phosphorylated $ERK^{T202/Y204}$ (197G2), AKT^{Thr308} (C31E5E), and ribosomal protein $S6^{Ser235/236}$ (D57.2.2E) were purchased from Cell Signaling Technology.

T cell stimulation

For phospho-flow assays, thymocytes or magnetic bead negatively purified peripheral $CD4^+$T cells were rested in serum-free medium for 30 min at 37°C, after which they were stimulated with 10 μg/ml of anti-CD3 (clone 2C11; University of California San Francisco [UCSF] Cell Culture Facility), followed by the addition of 50 ng/ml goat anti–Armenian hamster IgG (Jackson ImmunoResearch Laboratory) at 37°C for indicated times. For activation-induced cell death assays, such as intracellular Bim, thymocytes, or $CD4^+$ T cells were stimulated with plate-bound anti-CD3 Ab (2C11; 10 μg/ml unless otherwise indicated) and 2 μg/ml anti-CD28 Ab (clone 37.51; UCSF Cell Culture Facility) at 37°C for at least 16 h.

Intracellular staining

For phospho-ERK, -AKT, and -S6 staining, assays were performed as previously described (Hsu et al., 2009). Foxp3 and Egr2 staining was performed using the Foxp3 Staining Buffer Set (eBioscience). For intracellular staining of Bim, thymocytes were stimulated as described as in the preceding section and stained for surface markers before permeabilization using the Cytofix/Cytoperm kit (BD). Permeabilized cells were then stained with anti-Bim (clone C34C5) antibodies (Cell Signaling Technology), followed by staining with donkey anti–rabbit IgG-APC (Jackson ImmunoResearch Laboratory).

Calcium flux

Thymocytes or purified $CD4^+$ T cells from either OTII or W131AOTII mice were first surface-stained with anti–CD45.2-FITC and anti–CD45.2-PE, respectively, for subsequent identification of the two genotypes. Cells from both genotypes were mixed together, loaded with Indo-1 dye (Invitrogen) for 30 min at 37°C in RPMI medium plus 5% fetal bovine serum. After loading with Indo-1, cells were stained with CD4, CD8, Vα2, CD25, and TCRβ (for thymocytes) and CD44 (for peripheral T cells). Finally, cells were analyzed by flow cytometry (LSRFortessa [BD] with a UV laser) at 37°C and stimulated with 10 μg/ml anti-CD3, followed by cross-linking with 50 ng/ml goat anti–Armenian hamster IgG. Calcium increase was monitored as the ratio of Indo-1 (blue) and (violet) and displayed as a function of time.

Quantitative RT-PCR

Total RNA was purified using the RNeasy Micro kit (QIAGEN). cDNA was synthesized using Superscript III First-Strand Synthesis System (Invitrogen) according to the manufacturer's instructions. To measure the E3 ubiquitin ligase, GRAIL transcript level, TaqMan Real-Time PCR was performed using TaqMan Real-Time PCR Master Mix (Invitrogen) and TaqMan primer (primer 1: 5′-GCCAATTTC CTTGTCTCCTTG-3′, primer 2: 5′-CTGCTCGAAGAT TACGAAATGC-3′), and probe: 5′-/56-FAM/ACTGCC TCT/ZAN/GCTTCCTGCTTTGA/31ABkFQ/-3′ were purchased from IDT. An ABI Quantstudio machine (Applied Biosystems) was used for all quantitative PCR assays. The relative abundance of all target genes was normalized to the abundance of an internal reference gene (β2 microglobulin; β2m).

CD69 up-regulation and IL-2 secretion assay

Sorted naive $CD4^+OTII^+$ T cells ($CD4^+CD62L^{hi}CD44^{lo}$ $CD25^-V\alpha2^+$) were stimulated for 16 h at 37°C by TCR $C\alpha^{-/-}$ splenocytes preincubated with 1 μM OVA peptide. After overnight stimulation, IL-2–secreting $CD4^+$ T cells were identified using the IL-2 secretion assay (Miltenyi Biotec) according to the instructions of the manufacturer. In brief, cells were harvested and washed after stimulation, labeled with anti–IL-2 affinity matrix and incubated at 37°C with warm medium for 45 min. Captured IL-2, as well as CD69 and CD25 activation markers, were then detected simultaneously by flow cytometry with anti–IL-2-PE and anti-CD69, anti-CD25 antibody staining.

Bone marrow chimeras

Mixed bone marrow chimera was generated as previously described (Phee et al., 2010). In brief, equal numbers of T cell–depleted bone marrow cells from OTII ($CD45.1^+CD45.2^+$) and W131AOTII ($CD45.2^+$) mice were co-transferred into lethally irradiated BoyJ (CD45.1) recipient mice, and analyzed 8 wk post-transfer.

OVA immunization

Cell labeling and footpad injection were performed as previously described (Au-Yeung et al., 2014).

Anti–PD-1 mAb treatment

Treatment was performed as previously described (Fife et al., 2006). In brief, 4-wk-old OTII and W131AOTII mice were treated i.p. with 500 μg anti–PD-1 or control IgG on day 1 and with 250 μg every other day for 3 wk.

Statistical analysis

Unpaired two-tailed Student's *t* tests were performed to determine statistical significance between two groups.

ACKNOWLEDGMENTS

The authors thank J. Cyster and J. Zikherman for providing Bcl-2 and Nur77-eGFP tg mice, respectively; A. Ma for providing ES cells; J. Zikherman, B. Au-Yeung, R. Locksley, and M. Anderson for helpful suggestions; Z. Wang for cell sorting; A. Roque for animal husbandry; and K. Skrzypczynska for tail vein injections.

This work was supported by National Institutes of Health grants KO1 AR060807 (L.-Y. Hsu) and 2P01AI091580 (A. Weiss).

The authors declare no competing financial interests.

Author contributions: L.-Y. Hsu and A. Weiss designed the experiments. L.-Y. Hsu, D.A. Cheng, and Y. Chen performed the experiments. H.-E. Liang provided supports for ES cell culture. L.-Y. Hsu, and A. Weiss wrote the manuscript.

Submitted: 20 September 2016
Revised: 1 December 2016
Accepted: 12 December 2016

REFERENCES

Au-Yeung, B.B., J. Zikherman, J.L. Mueller, J.F. Ashouri, M. Matloubian, D.A. Cheng, Y. Chen, K.M. Shokat, and A. Weiss. 2014. A sharp T-cell antigen receptor signaling threshold for T-cell proliferation. *Proc. Natl. Acad. Sci. USA.* 111:E3679–E3688. http://dx.doi.org/10.1073/pnas.1413726111

Brdicka, T., T.A. Kadlecek, J.P. Roose, A.W. Pastuszak, and A. Weiss. 2005. Intramolecular regulatory switch in ZAP-70: analogy with receptor tyrosine kinases. *Mol. Cell. Biol.* 25:4924–4933. http://dx.doi.org/10.1128/MCB.25.12.4924-4933.2005

Cambier, J.C., S.B. Gauld, K.T. Merrell, and B.J. Vilen. 2007. B-cell anergy: from transgenic models to naturally occurring anergic B cells? *Nat. Rev. Immunol.* 7:633–643. http://dx.doi.org/10.1038/nri2133

Chan, A.Y., D. Punwani, T.A. Kadlecek, M.J. Cowan, J.L. Olson, E.F. Mathes, U. Sunderam, S.M. Fu, R. Srinivasan, J. Kuriyan, et al. 2016. A novel human autoimmune syndrome caused by combined hypomorphic and activating mutations in ZAP-70. *J. Exp. Med.* 213:155–165. http://dx.doi.org/10.1084/jem.20150888

Crespo, J., H. Sun, T.H. Welling, Z. Tian, and W. Zou. 2013. T cell anergy, exhaustion, senescence, and stemness in the tumor microenvironment. *Curr. Opin. Immunol.* 25:214–221. http://dx.doi.org/10.1016/j.coi.2012.12.003

Deindl, S., T.A. Kadlecek, T. Brdicka, X. Cao, A. Weiss, and J. Kuriyan. 2007. Structural basis for the inhibition of tyrosine kinase activity of ZAP-70. *Cell.* 129:735–746. http://dx.doi.org/10.1016/j.cell.2007.03.039

Deindl, S., T.A. Kadlecek, X. Cao, J. Kuriyan, and A. Weiss. 2009. Stability of an autoinhibitory interface in the structure of the tyrosine kinase ZAP-70 impacts T cell receptor response. *Proc. Natl. Acad. Sci. USA.* 106:20699–20704. http://dx.doi.org/10.1073/pnas.0911512106

Fife, B.T., I. Guleria, M. Gubbels Bupp, T.N. Eagar, Q. Tang, H. Bour-Jordan, H. Yagita, M. Azuma, M.H. Sayegh, and J.A. Bluestone. 2006. Insulin-induced remission in new-onset NOD mice is maintained by the PD-1-PD-L1 pathway. *J. Exp. Med.* 203:2737–2747. http://dx.doi.org/10.1084/jem.20061577

Hardy, J., and A. Singleton. 2009. Genomewide association studies and human disease. *N. Engl. J. Med.* 360:1759–1768. http://dx.doi.org/10.1056/NEJMra0808700

Heissmeyer, V., and A. Rao. 2004. E3 ligases in T cell anergy--turning immune responses into tolerance. *Sci. STKE.* 2004:pe29.

Hogquist, K.A., and S.C. Jameson. 2014. The self-obsession of T cells: how TCR signaling thresholds affect fate 'decisions' and effector function. *Nat. Immunol.* 15:815–823. http://dx.doi.org/10.1038/ni.2938

Hsu, L.Y., Y.X. Tan, Z. Xiao, M. Malissen, and A. Weiss. 2009. A hypomorphic allele of ZAP-70 reveals a distinct thymic threshold for autoimmune disease versus autoimmune reactivity. *J. Exp. Med.* 206:2527–2541. http://dx.doi.org/10.1084/jem.20082902

Imboden, J.B. 2009. The immunopathogenesis of rheumatoid arthritis. *Annu. Rev. Pathol.* 4:417–434. http://dx.doi.org/10.1146/annurev.pathol.4.110807.092254

Josefowicz, S.Z., L.F. Lu, and A.Y. Rudensky. 2012. Regulatory T cells: mechanisms of differentiation and function. *Annu. Rev. Immunol.* 30:531–564. http://dx.doi.org/10.1146/annurev.immunol.25.022106.141623

Kalekar, L.A., S.E. Schmiel, S.L. Nandiwada, W.Y. Lam, L.O. Barsness, N. Zhang, G.L. Stritesky, D. Malhotra, K.E. Pauken, J.L. Linehan, et al. 2016. $CD4^+$ T cell anergy prevents autoimmunity and generates regulatory T cell precursors. *Nat. Immunol.* 17:304–314. http://dx.doi.org/10.1038/ni.3331

Keir, M.E., Y.E. Latchman, G.J. Freeman, and A.H. Sharpe. 2005. Programmed death-1 (PD-1):PD-ligand 1 interactions inhibit TCR-mediated positive selection of thymocytes. *J. Immunol.* 175:7372–7379. http://dx.doi.org/10.4049/jimmunol.175.11.7372

Kishimoto, H., and J. Sprent. 1997. Negative selection in the thymus includes semimature T cells. *J. Exp. Med.* 185:263–271. http://dx.doi.org/10.1084/jem.185.2.263

Klammt, C., L. Novotná, D.T. Li, M. Wolf, A. Blount, K. Zhang, J.R. Fitchett, and B.F. Lillemeier. 2015. T cell receptor dwell times control the kinase activity of Zap70. *Nat. Immunol.* 16:961–969. http://dx.doi.org/10.1038/ni.3231

Mandl, J.N., J.P. Monteiro, N. Vrisekoop, and R.N. Germain. 2013. T cell-positive selection uses self-ligand binding strength to optimize repertoire recognition of foreign antigens. *Immunity.* 38:263–274. http://dx.doi.org/10.1016/j.immuni.2012.09.011

Moran, A.E., K.L. Holzapfel, Y. Xing, N.R. Cunningham, J.S. Maltzman, J. Punt, and K.A. Hogquist. 2011. T cell receptor signal strength in Treg and iNKT cell development demonstrated by a novel fluorescent reporter mouse. *J. Exp. Med.* 208:1279–1289. http://dx.doi.org/10.1084/jem.20110308

Mueller, D.L., and M.K. Jenkins. 1995. Molecular mechanisms underlying functional T-cell unresponsiveness. *Curr. Opin. Immunol.* 7:375–381. http://dx.doi.org/10.1016/0952-7915(95)80113-8

Odorizzi, P.M., and E.J. Wherry. 2012. Inhibitory receptors on lymphocytes: insights from infections. *J. Immunol.* 188:2957–2965. http://dx.doi.org/10.4049/jimmunol.1100038

Okazaki, T., S. Chikuma, Y. Iwai, S. Fagarasan, and T. Honjo. 2013. A rheostat for immune responses: the unique properties of PD-1 and their advantages for clinical application. *Nat. Immunol.* 14:1212–1218. http://dx.doi.org/10.1038/ni.2762

Pauken, K.E., and E.J. Wherry. 2015. SnapShot: T Cell Exhaustion. *Cell.* 163:1038–1038.e1. http://dx.doi.org/10.1016/j.cell.2015.10.054

Persaud, S.P., C.R. Parker, W.L. Lo, K.S. Weber, and P.M. Allen. 2014. Intrinsic $CD4^+$ T cell sensitivity and response to a pathogen are set and sustained by avidity for thymic and peripheral complexes of self peptide and MHC. *Nat. Immunol.* 15:266–274. http://dx.doi.org/10.1038/ni.2822

Phee, H., I. Dzhagalov, M. Mollenauer, Y. Wang, D.J. Irvine, E. Robey, and A. Weiss. 2010. Regulation of thymocyte positive selection and motility by GIT2. *Nat. Immunol.* 11:503–511. http://dx.doi.org/10.1038/ni.1868

Rodriguez-Manzanet, R., R. DeKruyff, V.K. Kuchroo, and D.T. Umetsu. 2009. The costimulatory role of TIM molecules. *Immunol. Rev.* 229:259–270. http://dx.doi.org/10.1111/j.1600-065X.2009.00772.x

Safford, M., S. Collins, M.A. Lutz, A. Allen, C.T. Huang, J. Kowalski, A. Blackford, M.R. Horton, C. Drake, R.H. Schwartz, and J.D. Powell. 2005. Egr-2 and Egr-3 are negative regulators of T cell activation. *Nat. Immunol.* 6:472–480. http://dx.doi.org/10.1038/ni1193

Sakaguchi, N., T. Takahashi, H. Hata, T. Nomura, T. Tagami, S. Yamazaki, T. Sakihama, T. Matsutani, I. Negishi, S. Nakatsuru, and S. Sakaguchi. 2003. Altered thymic T-cell selection due to a mutation of the ZAP-70 gene causes autoimmune arthritis in mice. *Nature.* 426:454–460. http://dx.doi.org/10.1038/nature02119

Schwartz, R.H. 2003. T cell anergy. *Annu. Rev. Immunol.* 21:305–334. http://dx.doi.org/10.1146/annurev.immunol.21.120601.141110

Sentman, C.L., J.R. Shutter, D. Hockenbery, O. Kanagawa, and S.J. Korsmeyer. 1991. bcl-2 inhibits multiple forms of apoptosis but not negative selection in thymocytes. *Cell.* 67:879–888. http://dx.doi.org/10.1016/0092-8674(91)90361-2

Sheppard, K.A., L.J. Fitz, J.M. Lee, C. Benander, J.A. George, J. Wooters, Y. Qiu, J.M. Jussif, L.L. Carter, C.R. Wood, and D. Chaudhary. 2004. PD-1 inhibits T-cell receptor induced phosphorylation of the ZAP70/CD3zeta signalosome and downstream signaling to PKCtheta. *FEBS Lett.* 574:37–41. http://dx.doi.org/10.1016/j.febslet.2004.07.083

Siggs, O.M., L.A. Miosge, A.L. Yates, E.M. Kucharska, D. Sheahan, T. Brdicka, A. Weiss, A. Liston, and C.C. Goodnow. 2007. Opposing functions of the T cell receptor kinase ZAP-70 in immunity and tolerance differentially titrate in response to nucleotide substitutions. *Immunity.* 27:912–926. http://dx.doi.org/10.1016/j.immuni.2007.11.013

Smith-Garvin, J.E., G.A. Koretzky, and M.S. Jordan. 2009. T cell activation. *Annu. Rev. Immunol.* 27:591–619. http://dx.doi.org/10.1146/annurev.immunol.021908.132706

Starr, T.K., S.C. Jameson, and K.A. Hogquist. 2003. Positive and negative selection of T cells. *Annu. Rev. Immunol.* 21:139–176. http://dx.doi.org/10.1146/annurev.immunol.21.120601.141107

van Oers, N.S., N. Killeen, and A. Weiss. 1994. ZAP-70 is constitutively associated with tyrosine-phosphorylated TCR zeta in murine thymocytes and lymph node T cells. *Immunity.* 1:675–685. http://dx.doi.org/10.1016/1074-7613(94)90038-8

Wang, H., T.A. Kadlecek, B.B. Au-Yeung, H.E. Goodfellow, L.Y. Hsu, T.S. Freedman, and A. Weiss. 2010. ZAP-70: an essential kinase in T-cell signaling. *Cold Spring Harb. Perspect. Biol.* 2:a002279. http://dx.doi.org/10.1101/cshperspect.a002279

Wherry, E.J., and M. Kurachi. 2015. Molecular and cellular insights into T cell exhaustion. *Nat. Rev. Immunol.* 15:486–499. http://dx.doi.org/10.1038/nri3862

Whiting, C.C., L.L. Su, J.T. Lin, and C.G. Fathman. 2011. GRAIL: a unique mediator of CD4 T-lymphocyte unresponsiveness. *FEBS J.* 278:47–58. http://dx.doi.org/10.1111/j.1742-4658.2010.07922.x

Witherden, D., N. van Oers, C. Waltzinger, A. Weiss, C. Benoist, and D. Mathis. 2000. Tetracycline-controllable selection of $CD4^+$ T cells: half-life and survival signals in the absence of major histocompatibility complex class II molecules. *J. Exp. Med.* 191:355–364. http://dx.doi.org/10.1084/jem.191.2.355

Yan, Q., T. Barros, P.R. Visperas, S. Deindl, T.A. Kadlecek, A. Weiss, and J. Kuriyan. 2013. Structural basis for activation of ZAP-70 by phosphorylation of the SH2-kinase linker. *Mol. Cell. Biol.* 33:2188–2201. http://dx.doi.org/10.1128/MCB.01637-12

Yokosuka, T., M. Takamatsu, W. Kobayashi-Imanishi, A. Hashimoto-Tane, M. Azuma, and T. Saito. 2012. Programmed cell death 1 forms negative costimulatory microclusters that directly inhibit T cell receptor signaling by recruiting phosphatase SHP2. *J. Exp. Med.* 209:1201–1217. http://dx.doi.org/10.1084/jem.20112741

Zikherman, J., R. Parameswaran, and A. Weiss. 2012. Endogenous antigen tunes the responsiveness of naive B cells but not T cells. *Nature.* 489:160–164. http://dx.doi.org/10.1038/nature11311